

Supporting Information

NMR Structural Studies on the Covalent DNA Binding of a Pyrrolobenzodiazepine-Naphthalimide Conjugate

Michael Rettig,^a Walter Langel,^a Ahmed Kamal,^b and Klaus Weisz^{a,*}

^a Institute of Biochemistry, Ernst-Moritz-Arndt-Universität Greifswald, Felix-Hausdorff-Str. 4, D-17487 Greifswald, Germany

^b Chemical Biology Laboratory, Division of Organic Chemistry, Indian Institute of Chemical Technology, Hyderabad 500607, India

Table of Contents

Figure S1: Base-H1' NOESY cross-peak spectral region of the free d(AACAATTGTT)₂ duplex in D₂O.

Table S1: Proton chemical shifts of d(AACAATTGTT)₂ in the 1:1 complex with the PBD-naphthalimide hybrid

Table S2: Proton chemical shifts of the free PBD-naphthalimide hybrid and in the 1:1 complex with d(AACAATTGTT)₂

Figure S2: Imino-imino and H1'-H3'/H4'/H5'/H5'' NOESY spectral regions of the complex in H₂O and in D₂O, respectively

Figure S3: Portion of a NOESY spectrum of the PBD-naphthalimide - d(AACAATTGTT)₂ complex in D₂O

Figure S4: H11a(ω_2)-H11(ω_1) and H11(ω_2)-H11a(ω_1) cross-peak structures of a DQF-COSY spectrum for the PBD-naphthalimide - d(AACAATTGTT)₂ complex

Figure S5: Aromatic region of a TOCSY spectrum and of a ROESY spectrum of the PBD-naphthalimide - d(AACAATTGTT)₂ complex in D₂O

Figure S6: Phase-sensitive 2D ³¹P-¹H HETCOR spectrum of the PBD-naphthalimide - d(AACAATTGTT)₂ complex

Table S3: ³¹P chemical shifts of free d(AACAATTGTT)₂ and in the 1:1 complex with the PBD-naphthalimide hybrid

Table S4: Helical parameters for the representative energy-minimized complex structure

Table S5: Glycosidic torsion angle κ and pseudorotation phase angle P with corresponding sugar pucker for the representative energy-minimized PBD-naphthalimide - d(AACAATTGTT)₂ complex

Figure S7: Distribution of NOE-derived intranucleotide and internucleotide distances within the DNA duplex

Fig. S1 Base-H1' NOESY cross-peak spectral region of the free d(AACAATTGTT)₂ duplex at 295 K (200 ms mixing time) in D₂O. The continuous network of intranucleotide and sequential H6/H8-H1' contacts starting with nucleotide 1 in 5'→3' direction is indicated by the solid lines.

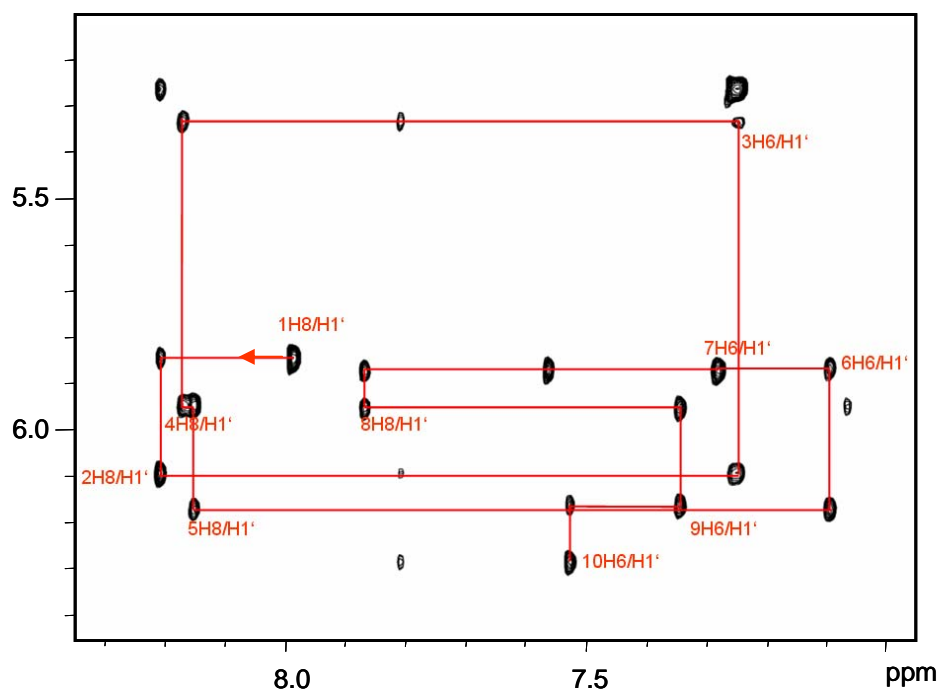


Table S1 Proton chemical shifts (ppm) of d(AACAATTGTT)₂ in the 1:1 complex with the PBD-naphthalimide hybrid at 298 K^a

proton	residue									
	A1	A2	C3	A4	A5	T6	T7	G8	T9	T10
H1'	5.845	6.04	5.215	6.19	6.20	5.815	5.685	4.95	6.085	6.30
H2'	2.37	2.675	1.53	2.745	2.605	2.07	2.36	2.09	2.20	2.32
H2''	2.525	2.735	2.02	2.745	2.94	2.43	2.52	2.765	2.385	2.32
H3'	4.815	4.985	4.635	5.125	4.955	4.81	4.92	4.915	4.945	4.605
H4'	4.175	4.39	4.05	4.395	4.54	4.285	4.29	4.24	3.72	4.105
H5'/H5''	3.685	4.13		4.13	4.24		4.115	4.035	3.955	4.20
		4.08		4.06	4.345				4.165	
H2		7.755			7.02					
H5			5.115							
H6			7.07			7.205	7.36		7.245	7.57
H8	7.955	8.175		7.98	8.36			7.84		
CH ₃						1.23	1.495		1.665	1.78
NH ^b						13.84	14.18	12.305	13.36	
NH ₂ (1) ^b			6.36		6.205			8.21		
NH ₂ (2) ^b			7.995							
proton	A11	A12	C13	A14	A15	T16	T17	G18	T19	T20
H1'	5.86	5.745	5.91	6.115	5.54	5.815	5.995	5.98	6.21	6.29
H2'	2.30	2.705	1.95	2.65	2.02	2.545	2.33	2.67	2.285	2.32
H2''	2.495	2.55	2.505	2.88	2.555	2.15	2.605	2.745	2.555	2.32
H3'	4.815	4.96	4.855	5.01	4.735	5.03	5.03	5.025	4.906	4.605
H4'	4.175	4.36	4.265	4.255	2.455	4.23	4.345	4.415	4.275	4.10
H5'/H5''	3.685	4.10	4.10	4.15	3.81	3.76	4.185			4.20
		4.04		4.11	3.86		4.005			
H2		7.81		7.285	7.725					
H5			5.365							
H6			7.275			7.33	7.565		7.405	7.57
H8	7.96	8.20		8.225	7.90			7.935		
CH ₃						1.455	1.925		1.555	1.765
NH ^b						12.145	12.88	12.22		
NH ₂ (1) ^b			5.995	6.53						
NH ₂ (2) ^b			7.815							

^a uncertainty ± 0.005 ppm. ^b NH₂(1) and NH₂(2) denote non-hydrogen and hydrogen-bonded amino protons. ^c H5' and H5'' resonances could not be unambiguously distinguished.

Table S2 Proton chemical shifts (ppm) of the free PBD-naphthalimide hybrid and in the 1:1 complex with d(AACAATTGTT)₂ at 298 K^a

proton	free ligand ^b	1:1 complex	proton	free ligand ^b	1:1 complex
1a/b	2.29	2.235/2.30	13a/b	4.08/4.13 ^c	3.88
2a/b	2.04	2.155/1.995	14	2.05	--
3a	3.56 ^c	3.665	15	2.56	--
3b	3.79 ^c	3.88	17/18/20/21	2.45-2.80	--
6	7.48	7.195	22	2.72	--
9	6.80	6.195	23	4.33	--
10	--	7.09	27/33	8.58	7.33/7.63 ^d
11	7.64	4.60	28/32	7.74	6.70/7.07 ^d
11a	3.70	5.16	29/31	8.19	7.65/-- ^d
12	3.91	3.985			

^a uncertainty ± 0.005 ppm. ^b In DMSO-d₆. ^c No stereospecific assignment for the two geminal protons. ^d no unambiguous assignment.

Fig. S2 (a) Imino-imino NOESY spectral region of the complex in H₂O (283 K, 200 ms mixing time); continuous sequential connectivities depicted by the horizontal and vertical lines start at base pair T9·G8 but are disrupted beyond base pair A5·T16. Except for the A5·T16 - A4·T17 step the absence of observable cross-peaks to the remaining base pairs must be attributed to the significant linebroadening of corresponding imino resonances at this temperature through solvent exchange. (b) H1'-H3'/H4'/H5'/H5'' NOESY spectral region of the complex in D₂O (298 K, 200 ms mixing time); strong contacts between drug H11 and H11a protons to DNA H1' protons are labeled.

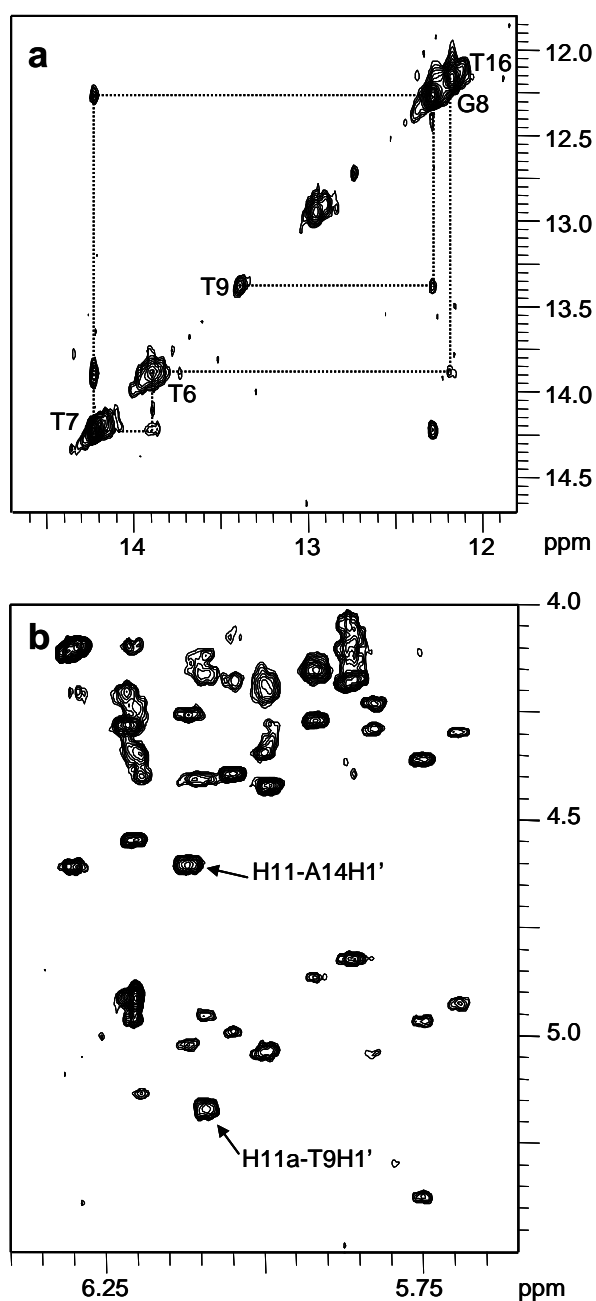


Fig. S3 Portion of a NOESY spectrum of the PBD-naphthalimide - d(AACAATTGTT)₂ complex in D₂O at 298 K (200 ms mixing time); intermolecular drug-DNA cross-peaks are labeled; circled cross-peaks of A15 and A5 H2 protons are attributed to NOE contacts with linker protons that could not be unambiguously assigned.

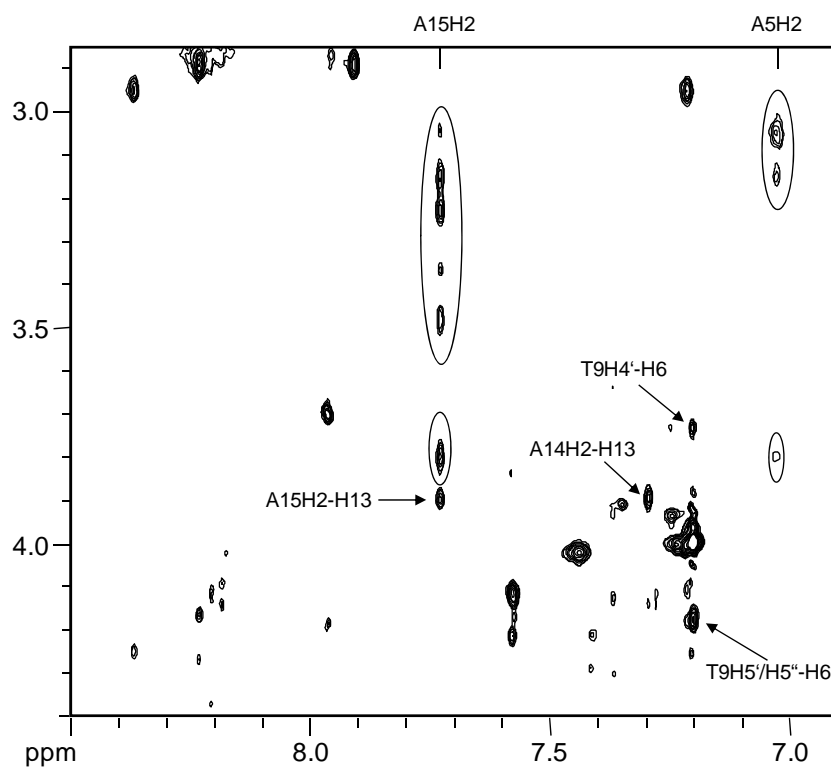


Fig. S4 H11a(ω_2)-H11(ω_1) (left) and H11(ω_2)-H11a(ω_1) cross-peak structures (right) of a DQF-COSY spectrum for the PBD-naphthalimide - d(AACAATTGTT)₂ complex in D₂O at 298 K. The spectrum was multiplied by a shifted sine square function in both dimensions prior to Fourier transformation and has a digital resolution of 1.1 and 2.2 Hz/point in ω_2 and ω_1 , respectively. Outer peak separation in the coupling fine structures along ω_2 correspond to sums of coupling constants $\Sigma J(\text{H11a}) = 18$ Hz and $\Sigma J(\text{H11}) = 10$ Hz. The additional passive coupling of H11a must be attributed to its vicinal coupling with an H1 proton of the pyrrolo ring giving rise to another H11a COSY cross-peak at the H1 chemical shift of 2.24 ppm (not shown). Taking into account amalgamation and cancellation effects, an estimate based on the peak separation of in-phase and antiphase components along ω_2 of corresponding cross-peaks yields coupling constants of $J(\text{H11a}, \text{H11}) = 10 \pm 0.5$ Hz and $J(\text{H11a}, \text{H1}\alpha) = 8 \pm 1$ Hz. Note, that another coupling between H11a and H1 β is expected to be rather small and only contributes to an increased signal linewidth.

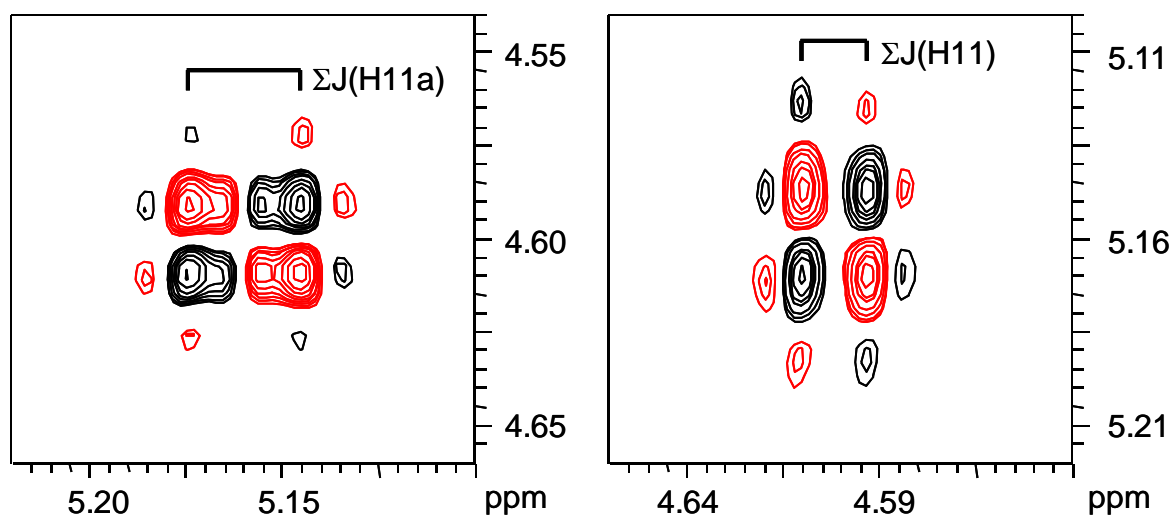


Fig. S5 (a) Aromatic region of a TOCSY spectrum (298 K, 100 ms mixing time) and of (b) a ROESY spectrum (293 K) of the PBD-naphthalimide - d(AACAATTGTT)₂ complex in D₂O, showing cross-peaks between significantly broadened spin-spin coupled resonances of the two naphthalimide spin systems (marked red and blue) and cross-peaks between pairs of exchanging, symmetrically disposed naphthalimide protons within the two separate spin systems, respectively. A missing exchange cross-peak between a third pair of symmetry-related naphthalimide protons is likely due to their similar chemical shift as is also indicated by the TOCSY correlations. Note, that at higher temperature the broadened naphthalimide protons finally disappear through their coalescence by exchange.

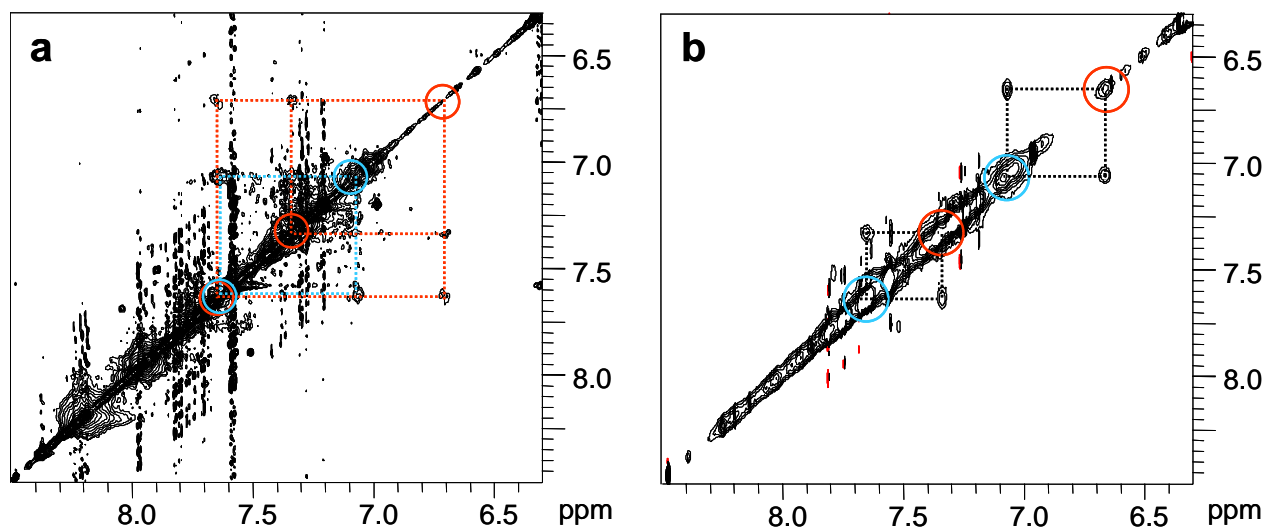


Fig S6 Phase-sensitive 2D ^{31}P - ^1H HETCOR spectrum of the PBD-naphthalimide - d(AACAATTGTT)₂ complex at 298 K with some selected cross-peaks labeled. Note the highly shielded A15H4' proton experiencing the largest upfield shift of all DNA protons upon drug binding.

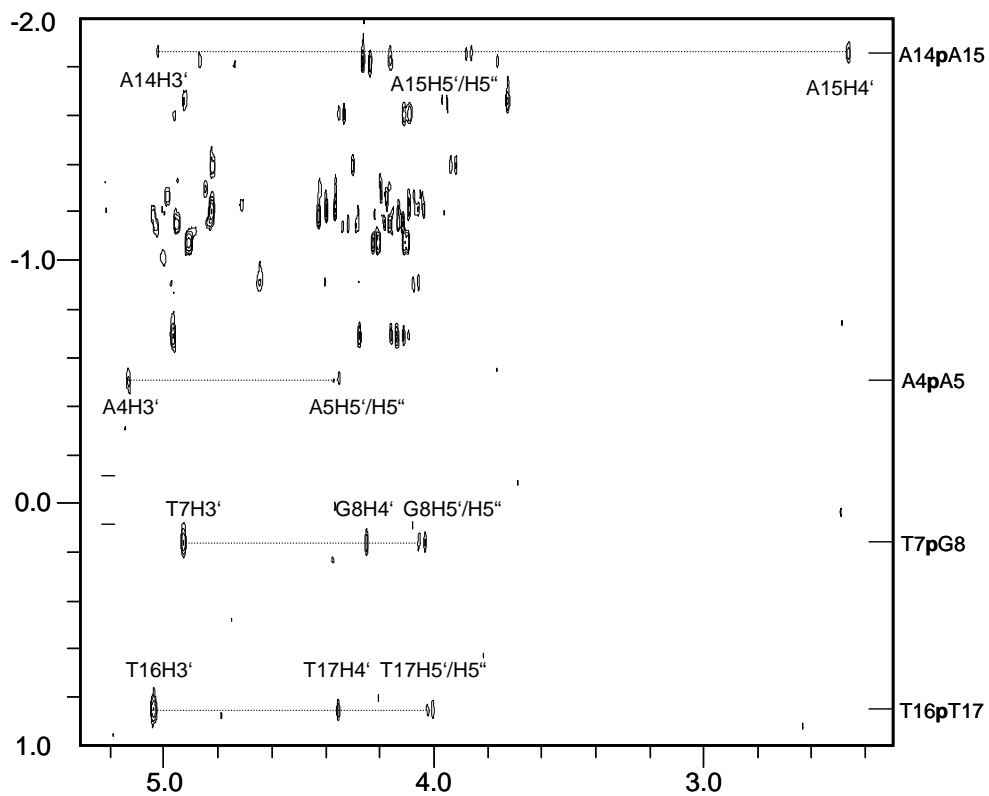


Table S3 ^{31}P chemical shifts (ppm) of $d(\text{ACAATTGTT})_2$ without and with the bound PBD-naphthalimide hybrid at 298 K^a

strand A	A1p	A2p	C3p	A4p	A5p	T6p	T7p	G8p	T9p
free duplex	-1.27	-1.44	-1.09	-1.42	-1.56	-1.52	-1.31	-1.29	-1.16
complex	-1.21	-1.27	-0.91	-0.51	-1.6	-1.4	0.16	-1.66	-1.15
strand B	A11p	A12p	C13p	A14p	A15p	T16p	T17p	G18p	T19p
duplex	-1.27	-1.44	-1.09	-1.42	-1.56	-1.52	-1.31	-1.29	-1.16
complex	-1.21	-0.69	-1.83	-1.86	-1.82	0.84	-1.19	-1.15	-1.08

^a uncertainty ± 0.01 ppm.

Table S4 Helical parameters^a for the representative energy-minimized complex structure^b

base pair	shear (Å)	stretch (Å)	stagger (Å)	buckle (deg)	propeller twist (deg)	opening (deg)
A2·T19	0.2	0.3	-0.6	5	-27	4
C3·G18	0.0	0.2	-0.3	1	-14	3
A4·T17	0.0	0.1	0.5	16	1	0
A5·T16	-0.2	0.2	-0.4	-15	0	-3
T6·A15	0.1	0.1	0.1	-7	-12	2
T7·A14	0.1	0.2	0.0	-1	-17	10
G8·C13	-0.4	0.1	-0.3	-7	-15	-2
T9·A12	-0.2	0.1	-0.4	-8	-22	-1
base pair step	shift (Å)	slide (Å)	rise (Å)	tilt (deg)	roll (deg)	twist (deg)
A2C3·G18T19	0.3	-0.9	3.2	-4	6	26
C3A4·T17G18	-0.1	-0.4	2.9	-6	5	29
A4A5·T16T17	0.8	0.7	7.4	11	-9	38
A5T6·A15T16	-0.3	-0.4	3.1	-6	0	27
T6T7·A14A15	0.4	-0.8	3.1	0	-3	31
T7G8·C13A14	-1.1	0.8	3.4	-6	-4	42
G8T9·A12C13	0.7	-0.4	3.2	-1	1	35

^a Individual parameters are defined with respect to a unique global helix axis. ^b Terminal base pairs were omitted.

Table S5 Glycosidic torsion angle κ and pseudorotation phase angle P with corresponding sugar pucker for the PBD-naphthalimide - d(AACAATTGTT)₂ complex (excluding terminal nucleotides)

nucleotide	A2	C3	A4	A5	T6	T7	G8	T9
κ	-85	-126	-115	-104	-120	-106	-114	-123
P	166	86	129	176	136	150	170	118
pucker	C2'-endo	O1'-endo	C1'-exo	C2'-endo	C1'-exo	C2'-endo	C2'-endo	C1'-exo
nucleotide	T19	G18	T17	T16	A15	A14	C13	A12
κ	-134	-94	-109	-101	-118	-105	-108	-93
P	104	139	165	140	107	155	142	143
pucker	O1'-endo	C1'-exo	C2'-endo	C1'-exo	O1'-endo	C2'-endo	C1'-exo	C1'-exo

Fig. S7 Distribution of intra-duplex NOE restraints among DNA residues.

